Determining the optimum installation of Energy Storage Systems in railway electrical infrastructures by means of swarm and evolutionary optimization algorithms

AUTHORS:

David Roch-Dupré, Tad Gonsalves, Asunción P. Cucala, Ramón R. Pecharromán, Álvaro J. López-López, Antonio Fernández-Cardador.

Abstract:

The installation of wayside Energy Storage Systems (ESSs) in DC-electrified railway systems is one of the main measures to improve their energy efficiency. They store the excess of regenerated energy produced by the trains during the braking phases and give it back to the system when necessary. Nevertheless, the big cost of the associated installation can make railway operators hesitate about the convenience of the investment. Additionally, the decisions about the configuration of the installation (locations and sizes for the ESSs) are usually based on the previous experience of the railway operators or, at best, in assessments made with simulation tools with low accuracy.

This paper proposes a model to optimize the profitability of the investment. Nature-inspired optimization algorithms are applied in combination with a very realistic railway simulator. The flexibility of the nature-inspired optimization algorithms, together with their ability to successfully deal with the computationally-intensive and highly non-linear and non-convex problem posed by the realistic railway simulator, makes them the perfect choice.

Three different nature-inspired optimization algorithms have been selected and compared: the Genetic Algorithm (GA) as the main exponent of the evolutionary algorithms, the Particle Swarm Optimization algorithm (PSO) as the main exponent of the swarm algorithms and the Fireworks Algorithm (FA) as another variant of the swarm algorithms. The algorithms have shown an excellent behavior, providing solutions that combine the increase of energy efficiency with a very good profitability of the installation required to obtain that increase.

Keywords: Nature-inspired optimization algorithms. Optimization of Energy Storage Systems. Railway power systems. Railway simulation. Energy efficiency.

1. Introduction

In the current context of looking for measures to mitigate climate change, improving the energy efficiency is crucial for DC-electrified railway systems. One of the possible strategies is to increase the utilization of the regenerated energy produced by trains during the braking phases [1]-[4]. In DC railway lines without infrastructure improvements, only trains that are motoring at the same instants when the regenerated energy is being produced can consume the regenerated energy. If this coordination between motoring and braking phases does not take place, the excess of regenerated energy must be dissipated in the rheostats (on-board resistors), which yields a considerable loss of energy efficiency. For this reason, it can be necessary to increase the receptivity of the system (its capability to accept regenerated energy) by installing infrastructure improvements, the main ones being:

- Reversible Substations (RSSs): they allow bidirectional power flows (from the utility grid to the catenary and vice versa) so that the excess of regenerated energy may be used in the operator's network or eventually sold back to the energy provider if the legislation allows it ([5]-[9]).
- Energy Storage Systems (ESSs): they store the excess of regenerated energy and give it back to the catenary when needed ([10]-[14]).

In recent years and nowadays, railway operators have shown a great interest in installing RSSs or ESSs to increase the energy saving in their lines. As stated in [15], these installations suppose a great investment that must be carefully assessed, usually with the help of simulation tools. However, the methodology to determine the optimal design of these installations is not sufficiently developed in scientific literature; decisions are usually made by means of unrealistic railway simulators or even based on the experience of railway operators.

Table 1 shows a summary of the state of the art on the application of methodologies for designing the improvements of the electrical infrastructure through the installation of RSSs and ESSs. All these studies use simulation tools and apply analysis or optimization techniques to provide a reasonable solution.

Regarding the studies in the literature that focus on the improvement of the infrastructure by the installation of RSSs, few of them deal with the problem of the optimal location and size. [16]-[20] use nature-inspired optimization algorithms. In particular [16]-[18] use the Genetic Algorithms (GA), while [19] uses the Immune Algorithm (IA) and [20] uses the Particle Swarm Optimization algorithm (PSO).

There are also a few works that study the optimal location and sizing for the ESSs. [21]-[23] use nature-inspired optimization algorithms. In particular, [22], [23] propose the Genetic Algorithm

(GA), while [21] proposes the Particle Swarm Optimization algorithm (PSO). There are also some authors who apply mathematical optimization models, such as the nonlinear optimization based on Lagrange multipliers (LGM) proposed by [24], [25], or the mixed integer linear programming (MILP) proposed by [26].

The decisions about the optimum infrastructure improvement that can be achieved with the installation of RSSs or ESSs highly depend on the accuracy of the railway simulator used together with the analysis or optimization techniques applied. Among the different modules of a railway simulator, the traffic model, although having a big impact on the results, has not been studied in detail in the literature. According to [15], an oversimplified traffic model can lead to considerable errors when computing the potential energy savings and, therefore, to wrong decisions about the infrastructure improvement to undertake.

Some of the most important traffic variables and features that must be taken into account for an accurate traffic model are provided in [15]: the headway (time interval between trains), the time shift (gap between the departure instant of trains in each direction from the terminal stations), the speed profiles of the trains and the traffic regulation system (which determines the most appropriate speed profile to be used by each train in each interstation). Besides, the traffic conditions also have a great impact on these traffic variables and features, as well as on the potential energy savings. According to [27], two main different traffic conditions must be distinguished: traffic with small perturbations and traffic with large perturbations. The perturbation is the deviation of train departures with respect to the commercial timetable and take place due to multiple causes:

- When the traffic has small perturbations, deviations are mainly due to small delays in the departure from the stations.
- When the traffic has large perturbations, deviations result in big delays, mainly due to the accumulation of trains in a certain track stretch.

Table 1 also shows the traffic variables and features contained in the studies previously presented. As can be seen, the vast majority of studies use simulations with very simplified traffic models. Only few of them use accurate traffic models, [6], [15], [27] being the most remarkable ones. [6] is the first example in the literature that observes most of the main traffic variables (the "synchronization delay" being a variable that includes the variability associated with the dwell time and the time shift). [15] is the first example with a complete model for traffic with small perturbations and [27] is the first example with a complete traffic model that observes both traffic conditions: small and large perturbations. Nevertheless, the focus of [15], [27] is only on analyzing the impact that the traffic model has on the estimation of the potential

energy savings obtained with the installation of RSSs. None of them tries to find the optimal configuration for the infrastructure improvements.

Table 1: Research works where the installation of RSSs or ESSs has been studied

RSSs / ESSs	Analysis / Optimization	Opt. Method	Traffic model					Reference
			Variable headway	Variable time-shift	Variable dwell time	Different speed profiles	Traffic regulation system	
RSSs	Optimization	GA	Yes	No	No	No	No	[16]
	Optimization	GA	No	No	No	No	No	[17]
	Optimization	GA	Yes	"stochastic operation" (without details)		No	No	[18]
	Optimization	IA	Yes			No	No	[19]
	Analysis	-	No	No	No	No	No	[28]
	Analysis	-	Yes	No	No	Yes	Yes	[29]
	Optimization	PSO	Yes	Yes	Yes	No	No	[20]
	Analysis	-	Yes	"sychronization delay"		Yes	No	[6]
	Analysis	-	Yes	Yes	Yes	Yes	Yes	[15]
	Analysis	-	Yes	No	Yes	Yes	Yes	[27]
ESSs	Optimization	GA	Yes	No	No	No	No	[23]
	Optimization	GA	No	No	No	No	No	[30]
	Optimization	LGM	No	No	No	No	No	[24]
	Optimization	LGM	No	No	No	No	No	[25]
	Optimization	MILP	No	No	No	No	No	[26]
	Optimization	PSO	No	No	No	No	No	[21]
	Analysis	-	Yes	No	No	No	No	[10]
	Analysis	-	Yes	No	Yes	No	No	[13]

Therefore, this paper aims to fill this gap: determining the optimal configuration (number, location and size) to improve the infrastructure of a railway line with the help of a railway simulator with an accurate and realistic traffic model. The search for the optimum configuration will be made with several nature-inspired optimization algorithms as they have been proved to be very flexible and successful in dealing with computationally-intensive and highly non-linear and non-convex problems [31]-[33], such as the one presented by the realistic railway simulator that is going to be used. For this study, the infrastructure improvement will consist of the installation of ESSs. Nevertheless, the algorithms and methodology proposed in the paper can be also applied to find the optimal configuration for RSSs.

Regarding the structure of the paper, Section 2 describes the methodology. Section 3 formulates the optimization problem and explains the algorithms designed to solve it. Section 4 presents the case study. Section 5 gives the details about the way the algorithms have been applied. Section 6 contains the results. Finally, Section 7 has the main conclusions that can be drawn from this paper.

2. Methodology

2.1. Railway simulator

Although the thorough description of the railway simulator used for this research is out of scope of this paper, it must be noted that it is very detailed, both from the electrical and traffic modelling points of view. Figure 1 provides a graphical explanation of the railway simulator. A simplified description of the main steps of the simulation process is given below (it is based on the explanations provided by [15], [27]:

1. *Step 1*: Creating the traffic scenarios that contains the power consumption and regeneration profiles of each train at each time instant and location of the railway line. This process requires:

   a. A **train movement simulator** that generates the speed, power consumption and regeneration profiles of a train. It is divided into three main modules [34], [35]:

      - **The train module** takes into account train's characteristics: length, mass, running resistance and rotary inertia. The motor features are also observed with the maximum traction and braking effort curves as a function of the train speed and the efficiency as a function of the effort ratio and train speed. No effects on train dynamics due to pantograph voltage variations are taken into account, and hence the results of the mechanical simulation of the system are not affected by electrical results. This assumption is made taking into account common features of modern traction equipment [36] and that metro lines are not subject to interoperability regulations.

      - **The line module** includes the physical information of the track: grades, grade transition curves (and the effect along the train), bends, bend transition curves and tunnels. Additionally, it includes the operational characteristics of the track such as permanent and temporary speed limits.

      - **The Automatic Train Operation (ATO) module** represents the control logic of the train automatic driving. Based on train's speed and position and considering the speed limits and the programmed driving commands, the ATO computes the value of traction/braking command to be sent to the motor.

   b. The **traffic model**, which observes the two main traffic conditions: traffic with small and large perturbations. Several headway values are used in order to take into account the different situations that take place during the day (peak hours, off peak hours, etc.). The values and characteristics of the rest of the traffic variables and features previously described are determined by the **realistic traffic module** and will depend on the traffic conditions:

- **Model for traffic with small perturbations**: noise associated with different types of uncertainties is added to the time shift and to the dwell time (modelled according to a log-normal distribution [37]). There is also a traffic regulation system in charge of selecting the most appropriate speed profile by finding the best balance between punctuality and energy consumption reduction: if the train departs with some delay from a station (with respect to the commercial timetable), a faster and more energy-consuming speed profile than the one used in the commercial timetable is selected, while if the train from a station departs in advance (with respect to the commercial timetable), a slower and less energy consuming speed profile than the one used in the commercial timetable is selected. The detailed explanation of the model for **traffic with small perturbations** is given in [15].

- **Model for traffic with large perturbations**: as trains are accumulated in certain track stretches due to large perturbations, their speed profile is affected by the signalling system, in order to separate it from the previous train (the perturbations on the speed profile can go from activating speed limits to making intermediate stops). Dwell times are also affected as the signalling system might not allow the departure of a train from a station if there is another train stopped in the vicinity. The detailed explanation of the model for **traffic with large perturbations** is given in [27].

Contrary to what usually happens in the literature, the output from the traffic model is not a single traffic scenario per headway, but a large number of different traffic scenarios, where all the variability associated with the different traffic variables and features previously explained is observed. This variability due to the traffic is proven to have a high impact on the assessment of the infrastructure improvements [15], [27].

2. *Step 2*: Integrating the train traffic timetable within the electrical infrastructure to generate the equivalent electrical scenarios that must be solved (each time sample has an associated electrical scenario/circuit, called "snapshot"). The **electrical scenario generator** is in charge of this task and its details can be found in [38].

3. *Step 3*: Solving the load flow of all the electrical scenarios in the **load flow module**. Each snapshot is non-linear and must be solved with the application of iterative techniques. In particular, the iterative technique used by the simulator is the unified-mixed AC-DC Newton-Raphson method (for more details see [38]), which calculates:

- Voltages and angles in AC nodes (e.g: the AC nodes of the traction substations).
- Voltages in DC nodes (e.g: the DC nodes of the tractions substations, train pantographs, catenary nodes, etc.).

After solving the load flow, all the electrical variables are computed, among them: power

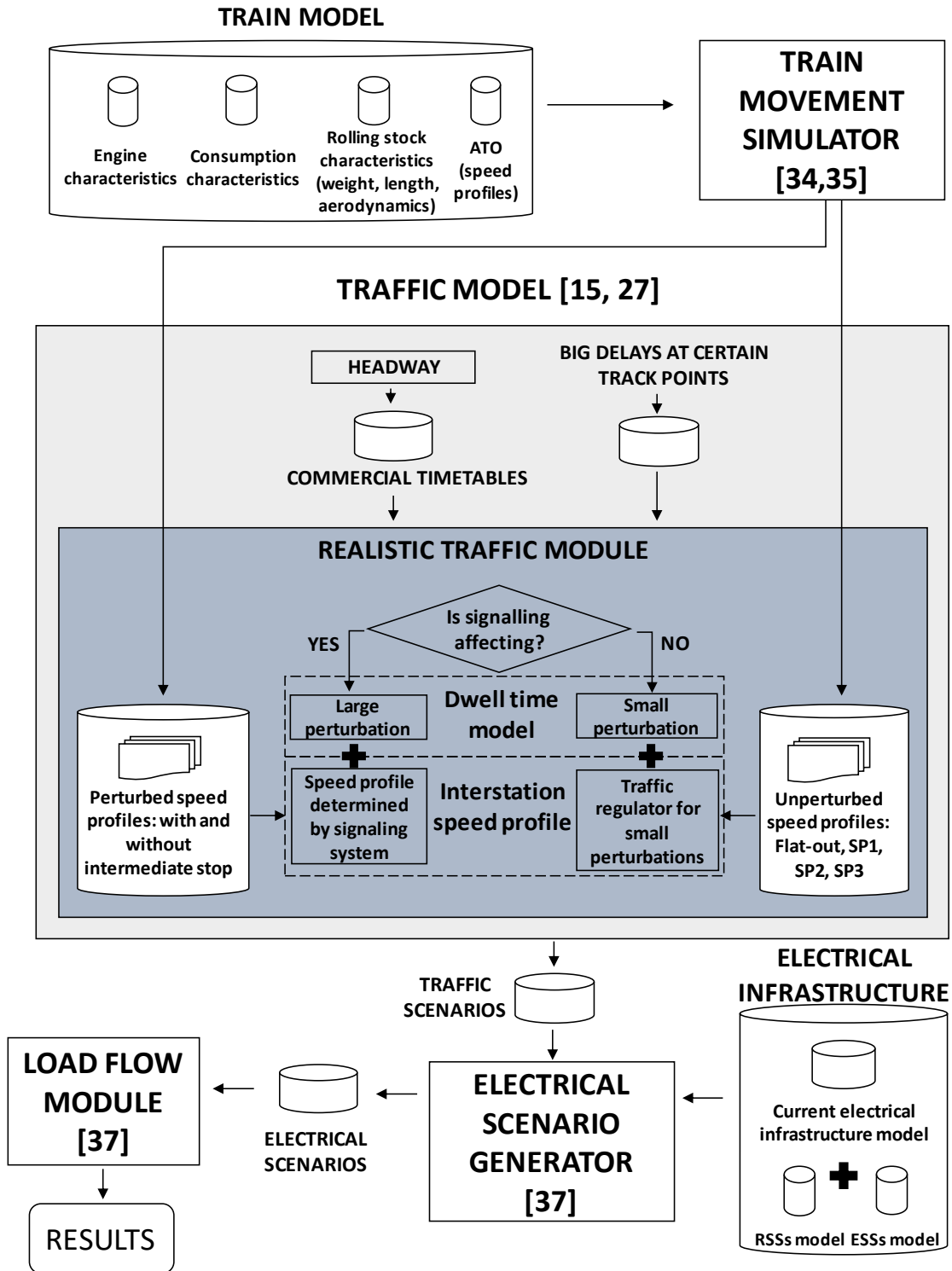consumption in substations, rheostat losses, grid losses, etc.

TRAIN MODEL

Figure 1: Railway simulator [27]

4. _**Step 4:**_ Selecting the electrical variables of interest and performing the required

   computations, that can vary depending on the objective of the simulation. In the case of this

   paper, the variable used as input for the optimization algorithms looking for the optimal

location and size of the ESSs is the energy consumption in the substations.

For the sake of clarity, the railway simulator can be divided in two main parts:

- *__Operation module__*: is in charge of step 1 and includes the **train movement simulator** and the **traffic model**.
- *__Electrical network module__*: is in charge of steps 2, 3 and 4 and includes the **electrical scenario generator** and the **load flow module**

2.2. Communication between the optimization algorithms and the railway simulator

With the information provided by the electrical simulation, the next step is to decide which, among all the possible configurations for the infrastructure improvements, produces the best result (in terms of profitability and energy saving, as will be explained in Section 3). The attributes of each configuration are the following:

- Number of ESSs to install.
- Location of the ESSs to install.
- Power (kW) of the ESSs to install.

It must be noted that the energy storage capacity of the ESSs will be set to 5 kWh. Although it is clear that the higher the capacity, the higher the energy saving, this value allows -for the case-study railway line concerning this paper- not losing significant amounts of regenerated energy due to lack of storage capacity. It has not been included in the formulation of the optimization problem as a variable of decision because its impact is very low compared to the power (the cost associated with the power of the ESS is more than 10 times higher than the cost associated with the capacity). In future works this variable will be also considered as a variable of decision.

The communication process between the algorithm and the simulator is made up of the following steps:

1. The algorithm gives the configuration (locations and power) of the ESSs installations to be tested as the input data for the simulator.
2. The electrical network module simulates each ESSs configuration provided by the algorithm in the different traffic scenarios generated by the operation module. After performing the electrical simulations, the energy saving associated with this configuration is given as the output data to the optimization algorithm.
3. The Net Present Value of each configurations is computed from its associated energy saving and installation cost (see Section 3.1 to see the way NPV is computed) and the optimization algorithm will use it as the fitness value of the optimization problem.

3. Optimization

The optimization algorithms will try to find the optimum ESSs configuration (regarding number, location and power size). This paper will use nature-inspired optimization algorithms instead of using formal mathematical models. The main reasons for this choice are explained in [20]:

- Formal optimization models must solve a highly non-linear and non-convex load flow problem, while deciding the optimal configuration of the electrical infrastructure. This causes very complex and time-consuming optimization processes.
- Formal optimization models use a large number of simplifications for the traffic model, which does not ensure that they are capable of dealing with complex metropolitan lines, where there are different time intervals between trains and many possible traffic scenarios.

The three optimization algorithms selected are the Genetic Algorithm (GA) [39], the Particle Swarm Optimization Algorithm (PSO) [40] and the Fireworks Algorithm (FA) [41]. The GA and the PSO are, respectively, the main exponents of the evolutionary and swarm algorithms and have been used in multiple applications [42], [43]. The FA is an interesting and novel proposal within the swarm algorithms with promising results [44]. The optimization problem will be defined in Section 3.1, while the particular implementation of each algorithm will be explained in Section 3.2.

3.1. Optimization problem

In order to fit with this optimization problem, the standard GA, PSO and FA have been reformulated as knapsack problems with some changes. The knapsack problem is a well-known problem found in the optimization literature [45] and consists in picking and choosing a set of items from a given larger set to put in the knapsack so as to maximize the total value, under the weight constraints of the knapsack. The knapsack optimization problem is generally coded as a bit string containing zeros and ones – a "one" representing the fact that a certain item is selected and a "zero" representing the fact that a certain item is not selected. For the particular case of this optimization problem, each item represents one of the potential locations where an ESS can be installed and, instead of having a bit string containing zeros and ones, each item has a value from a set of discrete values that represent the possible amounts of power that can be installed. The weight constraints are related to the maximum admissible budget that cannot be exceeded.

Therefore, each chromosome (in the case of the GA), particle (in the case of the PSO) or spark (in the case of FA) contains the characteristics of one ESSs' configuration according to the structure given by (1):

$$p_i = [pow_1, pow_2, \cdots pow_k \cdots pow_N] \tag{1}$$

Where:

- ✓ pow_k is the item associated with position k and represents the power (kW) for the ESS installed in that position. The values for this variable are discrete, going from 0 kW (no ESS installed in position k) to max_{pow} kW (maximum power that can be installed) in steps of $step_{pow}$ kW. Therefore, each item must take one value out of the available set of $\frac{max_{pow}}{step_{pow}}$ discrete values (being max_{pow} a multiple of $step_{pow}$).

- ✓ N is the number of potential locations for installing the ESS. This means that each chromosome/particle/spark will have N items.

The optimal solution is the one that yields the highest Net Present Value (NPV) of the installation. Therefore, the fitness function for a given chromosome/particle/spark i (p_i) is the NPV of its associated ESSs configuration. The equation of the fitness function is in (2).

$$NPV(p_i) = \sum_{t=1}^{T} \frac{\left(E_{Raw}^{ANNUAL} - E_{ESSs}^{ANNUAL}(p_i)\right) \cdot e_{cost}}{(1 + wacc)^t} - C_0(p_i) \tag{2}$$

$$s.t \quad C_0(p_i) \leq budget$$

Where:

- ✓ E_{Raw}^{ANNUAL} is the annual energy consumption without any infrastructure improvement. This value is obtained from the railway simulator.

- ✓ $E_{ESSs}^{ANNUAL}(p_i)$ is the annual energy consumption obtained with the ESSs configuration determined by the spark p_i. This value is obtained from the railway simulator.

- ✓ e_{cost} is the energy price. This parameter allows transforming the energy saving, which is computed by comparing the total energy consumption with and without infrastructure improvement $\left(E_{Raw}^{ANNUAL} - E_{ESSs}^{ANNUAL}(p_i)\right)$ into economic cash flows.

- ✓ $C_0(p_i)$ is the installation cost of the ESS configuration determined by chromosome/particle/spark i (p_i).

- ✓ $wacc$ is the Weighted Average Cost of Capital.

- ✓ T is the period to evaluate the investment.

- ✓ $budget$ is the maximum amount of money available to undertake the infrastructure improvement.

The reason why the NPV has been selected as fitness function is that it is capable of finding a balance between what is important from the environmental point of view- the energy saving- and what is important for the railway operator –justifying the investment in the infrastructure improvement and obtaining economic benefits from it. The investment will be economically

profitable if the NPV is positive in T. Therefore, the optimization algorithms will try to determine the configuration with the highest NPV (the higher the NPV, the better the balance between the energy savings and the cost of the installation).

3.2. Implementation of the optimization algorithms

Sections 3.2.1, 3.2.2 and 3.2.3 provide the explanation of each algorithm. For a better understanding, Figure 2 shows the flow chart of the three of them.
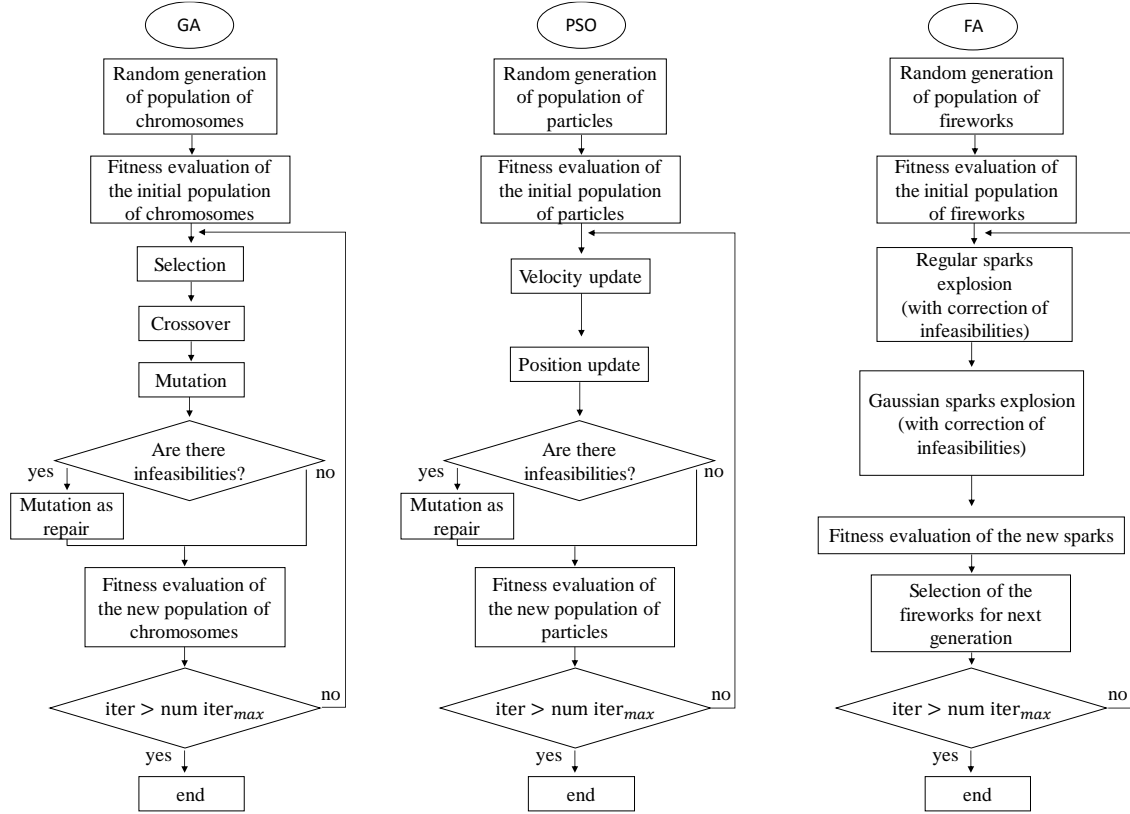
Figure 2: Flowchart of the GA, PSO and FA

3.2.1. Genetic Algorithm (GA)

The Genetic Algorithm (GA) is a well-known optimization metaphor based on the natural selection process. It begins with a population of random solutions called chromosomes, and evolves them through several cycles of selection, crossover and mutation operations. The better fit selected chromosomes exchange the promising genetic information, which is further mutated to give rise to ever evolving and best fit or optimal solutions.

Each chromosome has N items that can take one of the $\frac{max_{pow}}{step_{pow}}$ possible values, according to the knapsack formulation previously explained. In the case of the GA, each item will be called a gene. The steps of the GA are based on [45], listed below and depicted in Figure 2.

GA 1. Random generation of population of chromosomes: all the chromosomes are randomly generated and must not violate the budget constraints.

GA 2. Fitness evaluation of the initial population of chromosomes: the infrastructure configurations of the initial chromosomes are simulated in the railway simulator, which provides the energy saving associated with them. With this information and the cost of the installation associated with each chromosome, the NPV is computed by applying (2).

GA 3. Selection: the *tournament selection* procedure has been selected. A pair of chromosomes is randomly selected from the *children population* of the previous iteration or from the initial population in case of the first iteration. The fitness of both chromosomes are compared and the chromosome with the highest fitness is selected as a "parent chromosome" for the next generation. This selection procedure is repeated until the number of selected parents equals the population size and the same chromosome can be selected more than once (every pair is randomly selected from the whole *children population* of the previous iteration/initial population). After having the "parents" for the new population, one of them is randomly selected and replaced by the chromosome with the best fitness of the *children population* of the previous iteration /initial population. The population resulting from the selection will be called *parent population.*

GA 4. Crossover: two types of crossover mechanisms have been selected (each of them have been applied in a different optimization scenario, as will be seen in Section 5.2).

    a. ***One-point crossover***: parents are randomly selected in pairs as well as a single crossover point for each pair. The part of the chromosome after the crossover point is exchanged between the parents.

    b. ***Uniform crossover***: parents are randomly selected in pairs and each gene is swapped between each pair with a probability p_{swap}.

The population resulting from the crossover will be called *children population.*

GA 5. Mutation: every chromosome of the *children population* can be modified in one of its genes with a probability mut_1, in two of them with a probability mut_2 or in none of them with a probability mut_0. The relationship among probabilities mut_2, mut_1, mut_0 is shown in (3).

$$mut_2 < mut_1 \ll mut_0$$
$$mut_1 + mut_2 + mut_0 = 1 \tag{3}$$

GA 6. Fitness evaluation of the new population of chromosomes: the chromosomes of the *children population* are evaluated in the same way as the described in step 2 (**GA 2**). Once the new fitness values are obtained, the algorithm proceeds to the next iteration,

which starts in step **GA 3**. This process is repeated for a number of iterations given by $num\ iter_{max}$.

The *children population* is obtained from the *parent population* after applying the crossover and mutation mechanisms. It may happen that some chromosomes of the *children population* are not feasible as their installation cost is higher than the maximum budget. In order to avoid infeasibilities, the **mutation as repair** mechanism is applied to those chromosomes. This mechanism consists in randomly selecting genes with non-zero values and reducing its size in $step_{pow}$ (the minimum admissible change in size) until the installation cost of the chromosome becomes feasible.

3.2.2. Implementation of the Particle Swarm Algorithm (PSO)

The Particle Swarm Optimization (PSO) is a metaphor in the swarm intelligence paradigm. It has become a popular meta-heuristic algorithm in the optimization domain and has been successfully applied to optimization problems ranging from business, engineering, healthcare, etc. Based on the food-gathering behavior of swarms of bees, birds and schools of fish, PSO optimally balances exploration and exploitation. Simplicity in implementation, negligible computational overhead and rapid convergence have made it one of the outstanding swarm intelligence paradigms.

Each particle maintains a history of its flying over the search space. In every cycle of flying, the swarm also records two important pieces of information – *pbest* (the best position found by a particle in the course of flying) and *gbest* (the best position found by the swarm as a whole). These two values act as beacons to guide the flying of the rest of the particles towards the global optimum during the search.

Unlike the GA, which is designed for discrete search spaces, the PSO was originally designed to deal with continuous search spaces. Nevertheless, the formulation of the PSO as a knapsack problem allows it to successfully deal with discrete search spaces. According to this reformulation, each particle of the population has N items that can take $\frac{max_{pow}}{step_{pow}}$ possible values.

In the case of the PSO, the position of the particle in a given iteration will be defined by the value taken by each of its N items. The steps of the PSO, according to [45], are listed below and depicted in Figure 2.

  PSO 1. Random generation of population of particles: same as the GA.

  PSO 2. Fitness evaluation of the initial population of particles: same as the GA.

  PSO 3. Velocity update: each particle has a position change known as velocity. In a given iteration, $iter$, the velocity of each particle is updated according to (4):

$$v(iter) = w \cdot v(iter - 1) + c_1 \cdot r_1 \cdot \big(pbest - x(iter - 1)\big) + c_2 \cdot r_2 \cdot \big(gbest - x(iter - 1)\big) \qquad (4)$$

Where:

- ✓ v is a vector of N items that determines the velocity of the particle.
- ✓ x is a vector of N items that determines the position of the particle.
- ✓ w is the inertia weight.
- ✓ c_1, c_2 are called social factors (being c_1 the personal attractor and c_2 the global attractor).
- ✓ r_1, r_2 are random numbers between 0 and 1.

PSO 4. Position update: in a given iteration $iter$, the position of each particle is updated according to (5). The values of each of the items of the particle obtained from updating the position are rounded to the nearest discrete value from the set of possible values.

$$x(iter) = v(iter) + x(iter - 1) \qquad (5)$$

PSO 5. Fitness evaluation of the new population of particles: the new particles are evaluated in the same way as the described in step 2 (**PSO 2**). Once the new fitness values are obtained, the algorithm proceeds to the next iteration, which starts in step **PSO 3**. This process is repeated for a number of iterations given by $num\ iter_{max}$.

As happened with the GA, some particles with the updated position may be not feasible. In order to avoid infeasibilities, the **mutation as repair** mechanism explained for the GA is also applied to the PSO.

3.2.3. Implementation of the Fireworks Algorithm (FA)

The Fireworks Algorithm (FA) is a recent Swarm Intelligence optimization algorithm, which derives its inspiration from the fireworks exploding in the night sky. The algorithm generates random initial positions of N fireworks. The fireworks explode generating sparks, depending on their respective amplitudes. Fireworks with higher fitness values have a smaller explosion amplitude and a larger number of explosion sparks, while fireworks with lower fitness values have a larger explosion amplitude and a smaller number of explosion sparks. In addition, random sparks are also generated based on a Gaussian mutation process. A new population of n fireworks is selected at the end of each iteration. This may include the original fireworks, as well as the regular and Gaussian sparks. The elitist strategy is maintained by always inserting the current best location in the new population.

Like the PSO, the FA was originally designed to deal with continuous search spaces. Nevertheless, the formulation of the FA as a knapsack problem allows it to successfully deal with discrete search spaces. According to this reformulation, each spark of the population has N

items that can take $\frac{max_{pow}}{step_{pow}}$ possible values. In the case of the FA, the location of the spark in a given iteration is defined by the value taken by each of its N items, which will also be called dimensions of the spark (consequently, each spark will have N dimensions). Apart from the reformulation as a knapsack problem, some parts of the standard FA defined by [41] have been discretized. The steps of the discretized FA are listed below and depicted in Figure 2.

FA 1. Random generation of population of fireworks: same as the GA.

FA 2. Fitness evaluation of the initial population of fireworks: same as the GA.

FA 3. Regular sparks explosion: from each firework a variable number of regular sparks is set off. The explosion has the following steps:

FA 3.1. Selecting the number of regular sparks per firework: each firework has a different amount of regular sparks to set off, which directly depends on the fitness of the firework: the higher the fitness of the firework, the higher the number of regular sparks to set off from that firework. The number of regular sparks per firework is determined by (6).

$$number\_sparks_{fwi} = round\left(m \cdot \frac{fit_{fw_i} - fit_{WORST} + \varepsilon}{\sum_{j=1}^{n}(fit_{fw_j} - fit_{WORST}) + \varepsilon} \right) \tag{6}$$

Where:

- ✓ $number\_sparks_{fw_i}$ is the number of regular sparks to be set off from firework i (fw_i).
- ✓ n is the number of fireworks, which corresponds to the population size.
- ✓ m is a parameter to control the total number of regular sparks generated by the n fireworks.
- ✓ fit_{fw_i} is the fitness of firework i (fw_i).
- ✓ fit_{WORST} is the worst fitness of the n fireworks.
- ✓ ε is a very small constant used to avoid zero-division-error.

FA 3.2. Selecting the amplitude of explosion per firework: the amplitude of explosion of each firework depends directly on the fitness of the firework: the higher the fitness of the firework, the smaller the amplitude. The smaller the amplitude, the higher the exploitation, while the higher the amplitude, the higher the exploration. The amplitude of explosion of a firework is determined by (7).

$$Ac_{fw_i} = \frac{fit_{BEST} - fit_{fw_i} + \varepsilon}{\sum_{j=1}^{n}(fit_{BEST} - fit_{fw_j}) + \varepsilon} \tag{7}$$

Where:

- ✓ Ac_{fw_i} is the amplitude of explosion of firework i (fw_i).

✓ fit_{BEST} is the best fitness of the n fireworks.

The original formula for the amplitude of the explosion defined in (7) is applied to obtain a first continuous value, Ac_{fw_i} for firework i, which then will discretized into two possible values :

- $step_{pow}$ when Ac_{fw_i} is within the xth percentile of the smallest continuous radii (which is equivalent to be within the x% of fireworks with the best fitness).

- $2 \cdot step_{pow}$ when Ac_{fw_i} is out of the xth percentile of the smallest continuous radii (which is equivalent to be within the (100-x)% of fireworks with the worst fitness).

After this transformation from continuous to discrete, each firework i will have an associated discrete amplitude of explosion Ad_{fw_i}.

FA 3.3. Generating the regular sparks: each regular spark differs from the firework from which it is set off in z randomly selected dimensions, z being a random number that goes from 0 to the total number of dimensions of the spark. The algorithm to compute the change in dimension k of regular spark j, exploded from firework i, is defined by (8).

$$sp_j^k = fw_i^k + randsample([-Ad_{fw_i}:step_{pow}:+Ad_{fw_i}]) \tag{8}$$

Where:

✓ fw_i^k is the value for dimension k of firework i.
✓ sp_j^k is the value for dimension k of regular spark j.
✓ $randsample$ is a logical operator that randomly selects one of the values of vector $[-Ad_{fw_i}:step_{pow}:+Ad_{fw_i}]$ according to a uniform distribution.

If dimension k of regular spark j crosses the maximum or minimum limits in power, the maximum or minimum power, respectively, is set for dimension k of regular spark j.

If an increment in the power of dimension k of regular spark j makes the spark infeasible in terms of budget, that increment is reduced to a feasible increment in terms of budget (this mechanism emulates, somehow, the mutation as repair mechanism of the GA and the PSO and ensures that the new sparks comply with the budget).

FA 4. Gaussian sparks explosion: according to [41], in order to keep the diversity of sparks, another type of explosion must also be applied to set off a very reduced amount of sparks. This type of explosion is called "Gaussian Explosion" and is only applied to $m_{gaussian}$ number of sparks. Each Gaussian spark is set off from a different firework

and differs from it in z randomly selected dimensions, z being a random number that goes from 0 to the total number of dimensions of the spark, N, (the same as in the regular explosion). The algorithm to compute the change in dimension k of Gaussian spark g, exploded from firework i, is defined by (9).

$$
\begin{aligned}
&while\ coeff < 0 \\
&\quad coeff = Gaussian\ (1,1) \\
&end
\end{aligned} \tag{9}
$$

$$
spg_g^k = round\left(\frac{fw_i^k \cdot coeff}{minimum\ step}\right) \cdot minimum\ step
$$

Where:

- ✓ $coeff$ is the coefficient of "Gaussian Explosion". It must be noted that $coeff$ must not be negative because the power of the ESS cannot be negative, just 0 (which means no installation of an ESS in the location associated with dimension k).

- ✓ sp_g^k is the value for dimension k of Gaussian spark g.

If dimension k of Gaussian spark g crosses the maximum limit in power (in this case it is not possible to cross the minimum), the maximum power is set for dimension k of Gaussian spark g.

If an increment in the power of dimension k of Gaussian spark g makes the spark infeasible in terms of budget, that increment is reduced to a feasible increment in terms of budget (this mechanism emulates, somehow, the mutation as repair mechanism of the GA and the PSO and ensures that the new sparks comply with the budget).

FA 5. **Fitness evaluation of the new sparks:** the new sparks are evaluated in the same way as the described in the step 2 (**FA 2**).

FA 6. **Selection of the locations of fireworks for the next generation:** n new fireworks to set off the sparks of the next generation must be selected from the fireworks and sparks of the current generation. Among all the sparks and fireworks of the current generation, the one with the best fitness is directly selected. The $n - 1$ remaining fireworks are selected according to their distance to other locations in order to keep diversity among fireworks. For this optimization problem, distance measure is computed according to the Manhattan distance (sum of the absolute value of the differences in every dimension of the sparks/fireworks). The probability for firework/spark x of current generation to become a firework in the next generation is defined by (10).

$$
p(x) = \frac{R(x)}{\sum_{i=1}^n R(fw_i) + \sum_{j=1}^m R(sp_j) + \sum_{g=1}^{m_{gaussian}} R(sp_g)} \tag{10}
$$

Where $R(...)$ is the sum of the distances between the spark/firework selected and the rest of fireworks and sparks. In the case of firework/spark x, this value is computed according to (11).

$$R(x) = \sum_{\alpha=1}^{n}\sum_{k=1}^{N}|x^k - fw_{\alpha}^k| + \sum_{\beta=1}^{m}\sum_{k=1}^{N}|x^k - sp_{\beta}^k| + \sum_{\gamma=1}^{m_{gaussian}}\sum_{k=1}^{N}|x^k - sp_{\gamma}^k| \qquad (11)$$

Once the new fitness values are obtained, the algorithm proceeds to the next iteration, which starts in step **FA 3**. This process is repeated for a number of iterations given by $num\ iter_{max}$.

4. Case study

4.1. *Topological, electrical and rolling stock characteristics*

The case study line is inspired by a real Spanish metro line but with changes to the topology in order to make it more complex from the point of view of the decisions to take for improving the infrastructure. Figure 3 represents, in a simplified way, the topology of the case study line.
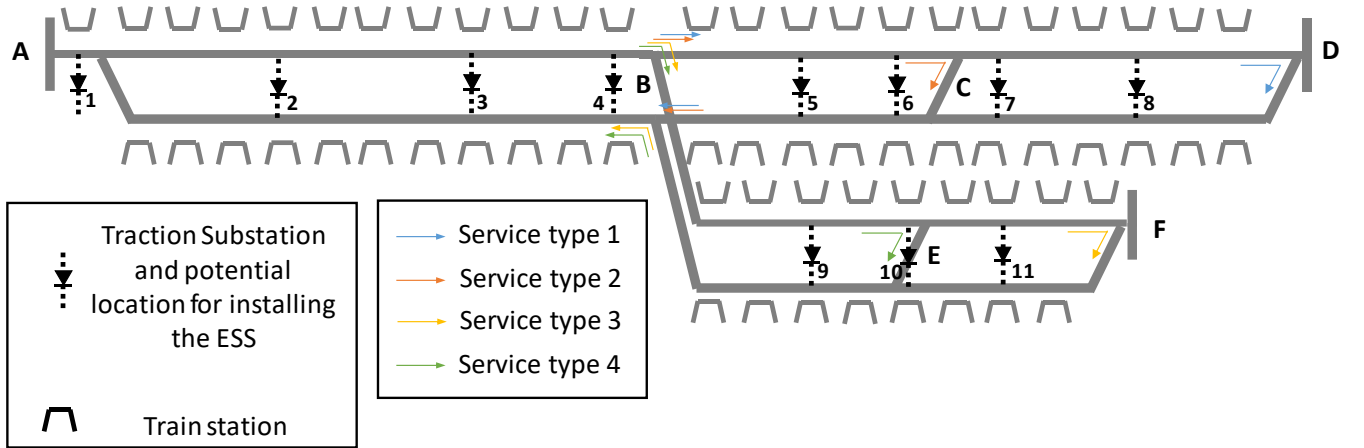
Figure 3: Case study line topology

As can be seen, there is a common section (section A-B), and two branches (branches B-D and B-F). Besides, each branch has two different terminal stations: (C and D for branch B-D; E and F for branch B-F). Therefore, there are four different types of train service:

- Type 1: the itinerary of the trains providing this type of service is A-B-C-D-C-B-A.
- Type 2: the itinerary of the trains providing this type of service is A-B-C-B-A.
- Type 3: the itinerary of the trains providing this type of service is A-B-E-F-E-B-A.
- Type 4: the itinerary of the trains providing this type of service is A-B-E-B-A.

The different types of service are repeated periodically in this order: Type 1- Type 4- Type 2- Type 3.

19

Table 2 shows the main electrical and topological characteristics of this line, as well as the information regarding the rolling stock.

Table 2: Case study topological, electrical and rolling stock characteristics

Topological and electrical and characteristics	Rolling stock characteristics
Line length. **Common section A-B:** 9.8 km **Branch B-D:** 10 km **Branch B-F:** 8.3 km **Maximum speed:** 70 km/h. **Passenger stations.** **Common section A-B:** 12 per track **Branch B-D:** 12 per track **Branch B-F:** 9 per track **Traction SSs:** 11 **Common section A-B:** 4 **Branch B-D:** 4 **Branch B-F:** 3 **Rectifier type (all SSs):** 6-pulse diode rectifiers (one-quadrant) **Rectifier nominal power.** **SSs 1-4 (common section):** 6.6 MVA. **SSs 5-11 (branches):** 4.8 MVA. **Nominal voltage of the line / No-load voltage:** 1600 / 1650 V **Feeder lines:** Conventional overhead conductor with a support feeder connected to the contact lines every 700 m (at these points, both track overhead conductor lines are paralleled). **Connectors on the feeding terminals of the traction power substation:** closed. The whole line is a single electrical sector. **Return circuit:** Both rails are used to carry the return current. **Total impedance of the active + return line:** 26 mΩ/km.	**Empty train mass:** 192.96 tons (only one type of train composition used). **Train maximum load:** 76.58 tons. **Train load in the study:** varies depending on the headway value from 25% of maximum load to 90% of maximum load (for more details see Section 4.2). **Type of braking:** Blend of pneumatic and electrical braking. The pneumatic braking is only used when the electrical braking is not able to provide the braking force commanded. **Electrical braking:** Regenerative. Trains feed braking power into the railway line if possible. If the maximum voltage is reached, the power surplus is sent to rheostats. **Maximum motoring power:** 5MW **Maximum regenerating power:** 4MW **Type of driving:** Automatic Train Operation (ATO) guided trains. **Auxiliary consumption power:** 200 kW. **Voltage threshold for the activation of the rheostatic braking:** 1800 V

Finally, the storage technology chosen consists in electrochemical double layer capacitors (EDLC) due to their good balance between its power and energy densities. The ESS management control will be according to the ESS control curve described in [13] and represented in Figure 4. It must be noted that the reference voltage value for defining the unitary units (p.u) is the no-load voltage: 1650 V.
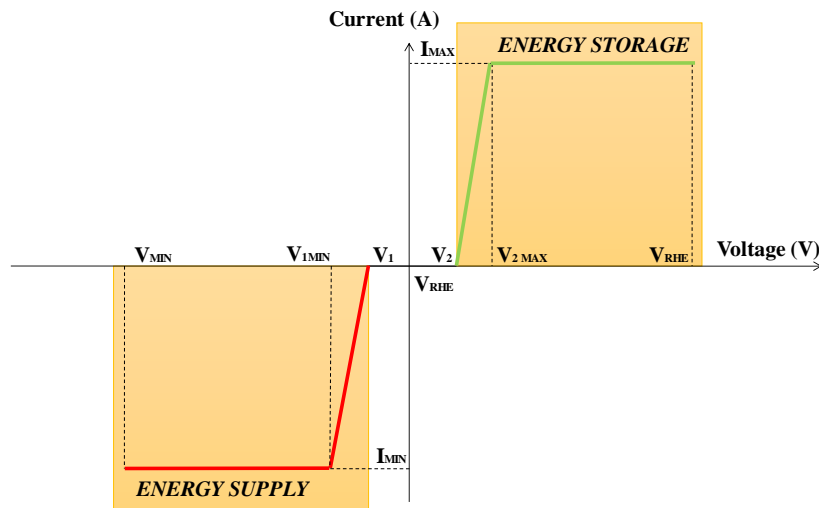
Figure 4: ESS control curve

Where:

- ✓ V_{RHE} is the voltage threshold for the activation of the rheostatic braking: 1800 V.
- ✓ V_{REF} is the reference voltage level, which coincides with the no-load voltage level: 1 p.u.
- ✓ V_1 is the voltage level at which the battery starts the discharging phase: 0.99 p.u.
- ✓ $V_{1\,MIN}$ is the voltage level at which the ESS reach its maximum discharging current (I_{MIN}): 0.95 p.u.
- ✓ V_2 is the voltage level at which the battery starts the charging phase: 1.01 p.u.
- ✓ $V_{2\,MAX}$ is the voltage level at which the ESS reach the maximum charging current (I_{MAX}): 1.05 p.u.
- ✓ V_{MIN} is the lower operating level of voltage: 0.66 p.u.

As can be seen, according to the values of the control curve parameters, both charging and discharging phases are activated as soon as possible, since their activation values, respectively determined by V_1 and V_2, are very close to the reference voltage. Therefore, and compared to other control curves that prioritize the voltage stabilization or the peak power shaving (where the value of V_1 is higher in order to preserve the stored energy for situations of voltage drops or power peaks), this control curve is designed to save the highest possible amount of energy.

4.2. Operation characteristics

In order to represent the different types of operation during the day in the case study line (peak hours, off peak hours, etc.), four different headway values have been chosen for the common section: 3, 5, 7 and 15 minutes. The headway value is the time interval between two consecutive trains. Therefore, the lower the headway, the higher the number of trains, the energy consumption and the regenerated energy.

Each traffic scenario represents the system operation during a long enough period. According to [15], the simulation length for each traffic scenario must be approximately the time required by a train to go from one terminal station to the other, in order to represent a typical operation cycle. For the case study line, as trains can give four different types of service, the simulation length has been defined as the time required by the longest service to go from one terminal station to the other, varying from 3700 secs to 6400 secs depending on the headway value. The simulation sample time is 1 second.

Simulations with large perturbations only take place at 3.5 min headway, while simulations with small perturbations take place at all the headway values. The distribution of the annual operation hours with each headway and perturbation type is depicted in Table 3.

<p align="center">Table 3: Main characteristics of the annual operation in the case study line</p>

	3.5 min with large perturbations	3.5 min with small perturbations	5 min with small perturbations	7 min with small perturbations	15 min with small perturbations
Hours of operation in a year	942.5	942.5	1885	2782	728
Percentage of total operation	12.95%	12.95%	25.9%	38.2%	10%

The train load varies depending on the headway value:

- At peak hours, represented by 3.5 and 5 min headways, the number of passengers is very high and train load is 90% of the maximum load.
- At off-peak hours, represented by 7 min headway, the number of passengers is lower and train load is 50% of the maximum load.
- At sparse traffic conditions, represented by 15 min headway, the train is almost empty, thus its load is 25% of the maximum load.

As explained in Section 2.1, this paper uses a very complete traffic model to properly represent real operation. As recommended in [27], in order to take into account the traffic variability associated with the traffic variables and features previously explained, a great amount of traffic scenarios with large and small perturbations has been generated. The variability among scenarios is associated with the different values that the main traffic variables can take (e.g: the dwell time), which directly affect the way the traffic regulation system (in the case of small

perturbations) or the signalling system (in the case of large perturbations) manage the traffic operation.

Additionally, when designing the commercial timetables (the original timetables for each headway from which the different traffic scenarios are generated by introducing variability in the traffic variables), different values of time-shift are used for operation with small perturbations (as stated in [27], this variable is not relevant for traffic scenarios with large perturbations). As there are four different types of service (see Section 4.1), the duration of a whole interval of operation is four times the headway value in the common section and, therefore, in order to properly take into account the variability associated with the time shift, 200 values equally separated and within the interval $[-headway \cdot 2, -headway \cdot 2)$ have been considered (in addition to the null-time shift, which is the most common in the literature).

5. Experimental design

5.1. Traffic scenarios reduction

Considering so much traffic variability (see Section 4.2) representing real operation results in a huge number of traffic scenarios. Trying to optimize the infrastructure with so many different traffic scenarios is very difficult and time consuming (as explained in Section 2.2, each infrastructure configuration tested by the optimization algorithm must be simulated in all the traffic scenarios generated by the operation module), so it is necessary to select the most representative traffic scenarios. The aim of selecting representative traffic scenarios is to obtain a reduced set of traffic scenarios which contains most of the information of the whole set of traffic scenarios. The selection of the representative traffic scenarios is based on [46], where a characterization of the traffic scenarios is performed based on the *Rheostat Loss Projection (RP)* function, which projects rheostat losses to a set of locations in the line. In the case of this paper, the set of locations is the set of N potential locations for installing the ESS. In addition, the *RP* function, which tries to compute the potential reductions in rheostat losses that can be achieved by increasing the receptivity (which in practice will be achieved with infrastructure improvements), has been replaced by the so-called *Single infinite Reversible Substation Test (SIRS-Test)*. The *SIRS-Test* computes the energy savings (directly correlated with the rheostat losses) obtained from installing "infinite" (no limit in power) Reversible Substations in the set of locations selected (one at a time). This test establishes the maximum amount of rheostat loss reductions that can be potentially achieved. The set of representative scenarios must have an error in the energy savings for all the locations tested in the *SIRS-Test* less than 5% with respect to the whole set of traffic scenarios. With these requirements, the number of scenarios has been reduced to 99%. To reduce the computational burden, the representative scenarios have been compressed according to [47].

Despite the selection and compression of the traffic scenarios, the computational burden is still quite considerable. Parallel computing has been used to speed up the optimization process: the ESSs configurations to be simulated in each iteration of any optimization algorithm have been distributed among a number of workers equivalent to the number of logical processors of the server. Two types of servers have been used:

- Server type 1:
  - CPU: AMD Ryzen Threadripper 2990WX , 32 Cores - 3000 MHz (64 logical processors).
  - RAM: 64 GB.
  - Disk: NVMe 512 GB.
- Server type 2:
  - CPU: Intel(R) Xeon(R) Silver 4116, 24 Cores-2100 MHz (48 logical processors).
  - RAM: 128 GB.
  - Disk: DELL PERC H330 1.65 TB.

The average simulation time required by these servers to perform the simulations associated with a single iteration of any optimization algorithm is around 40 minutes (having variations in time that mainly depend on the number of logical processors of the server).

5.2. Optimization cases and algorithms' parameters

Some general parameters (applicable to all the optimization algorithms) must be set for the variables of decision:

- **Location**: as can be seen in Table 2, there are 11 Traction Substations. The locations where the ESSs can be installed correspond to the locations of the Traction Substations. This choice is mainly due to operational reasons, since the installation and maintenance of the ESSs in these locations is much easier and simpler than in any other point of the line. Additionally, although installing the ESSs between Traction Substations can be better from the voltage regulation point of view, the case-study line does not have voltage drop problems. In consequence, every location of a Traction Substation is considered as a candidate to install the ESS: $N = 11$.
- **ESSs power**: this variable of decision can take any value among the set $[0: step_{pow}: max_{pow}]$, where:
  - $step_{pow} = 500 \, kW$
  - $max_{pow} = 3000 \, kW$

Although the search space of the optimization problem could be reduced by dividing the traction system in different sectors (which, for example, would reduce the number of potential

locations to install the ESSs in each sector), this approach is not possible because all the elements of the system are electrically connected.

Two optimization cases have been used for each algorithm in order to check their robustness and ten instances have been run for each algorithm in each case.

The two cases of the GA differ in the crossover mechanism used: the "*one-point crossover*" has been used for Case 1 and the "*uniform crossover*" has been used for Case 2. The parameters of the GA have been selected experimentally and are depicted in Table 4.

Table 4: GA parameters

	Case 1 (GA1)	Case 2 (GA2)
Population size (number of chromosomes)	128	
Probability for a chromosome to mutate one gene, mut_1	20%	
Probability for a chromosome to mutate two genes, mut_2	10%	
Probability to swap each gene among parents in the uniform crossover mechanism, p_{swap}.	-	50%
Maximum number of iterations, $num\ iter_{max}$	100	

The two cases of the PSO differ in the way the velocity is updated. In Case 1, the inertia weight, w, is a constant parameter, while in Case 2 it changes its value in every iteration according to the formula of the "*Linear Decreasing Inertia Weight*" proposed by [48] and defined in (12).

$$w(iter) = w_{max} - \frac{w_{max} - w_{min}}{iter_{max}} \times iter \tag{12}$$

Where:

- ✓ w_{max} is the maximum inertia weight.
- ✓ w_{min} is the minimum inertia weight.
- ✓ $iter$ is the current iteration.

The parameters of the PSO have been selected experimentally and are depicted in Table 5.

Table 5: PSO parameters

	Case 1 (PSO1)	Case 2 (PSO2)
Population size (number of particles)	128	
Inertia weight, w	0.5	$w_{max}=0.9$ $w_{min}=0.4$
Personal attractor, c_1	0.2	
Global attractor, c_2	0.3	
Maximum number of iterations, $num\ iter_{max}$	100	

The two cases of the FA differ in the proportion between fireworks and regular sparks. Maintaining the maximum number of sparks in both cases (the population of sparks in the FA is not constant but a maximum number of sparks must be set), the number of fireworks in Case 2 doubles the number of fireworks in Case 1 and, consequently, the average number of sparks per firework in Case 2 is half the average number of sparks per firework in Case 1.

The parameters of the FA have been selected experimentally and are depicted in Table 6:

Table 6: FA parameters

	Case 1 (FA1)	Case 2 (FA2)
Max. number of sparks	128	
Number of fireworks, n	13	26
x^{th} percentile to determine the radius of explosion	40	
Percentage of Gaussian sparks (against total number of sparks)	7%	
Maximum number of iterations, $num\ iter_{max}$	100	

5.3. Fitness function parameters

This section contains the values of the parameters used to calculate the fitness function as well as the reason why they have been chosen.

- e_{cost}: 0.0642 €/kWh. This is a realistic value obtained from the addition of the average energy price in Spanish market in the year 2018 and the energy tolls established by the Spanish Government for that year. For more details about the procedure to compute the energy cost, see [13].

- $C_0(sp_i)$: this value is computed by adding the total power and capacity installed and multiplying it by their unitary costs. The unitary costs for the EDLCs (the storage technology chosen for the ESSs) are depicted in Table 7 and have been obtained from the range of values proposed by [5].

**Table 7: Unitary costs for power and capacity**

Capital cost for energy [€/kWh]	Capital cost for power [€/kW]
270	90

- $wacc$: 2.5%. This is a reasonable interest rate.

- T: 15 years. This is a very reasonable estimation for the ESSs life according to the International Renewable Energy Agency (IRENA) [49].

- $budget$: for the case study, a budget of 280000 € has been selected, as it is flexible enough to allow a high number of different configurations to be installed, and restrictive enough so as not to allow very expensive configurations, which are not likely to be accepted by the railway operators. For real implementation, railway operators must set this value.

6. Results

6.1. Comparison of algorithms

Ten instances have been run for each optimization algorithm and case. Figure 5 shows the evolution of the average and the median of the fitness function for each algorithm and case in relation to the number of iterations.
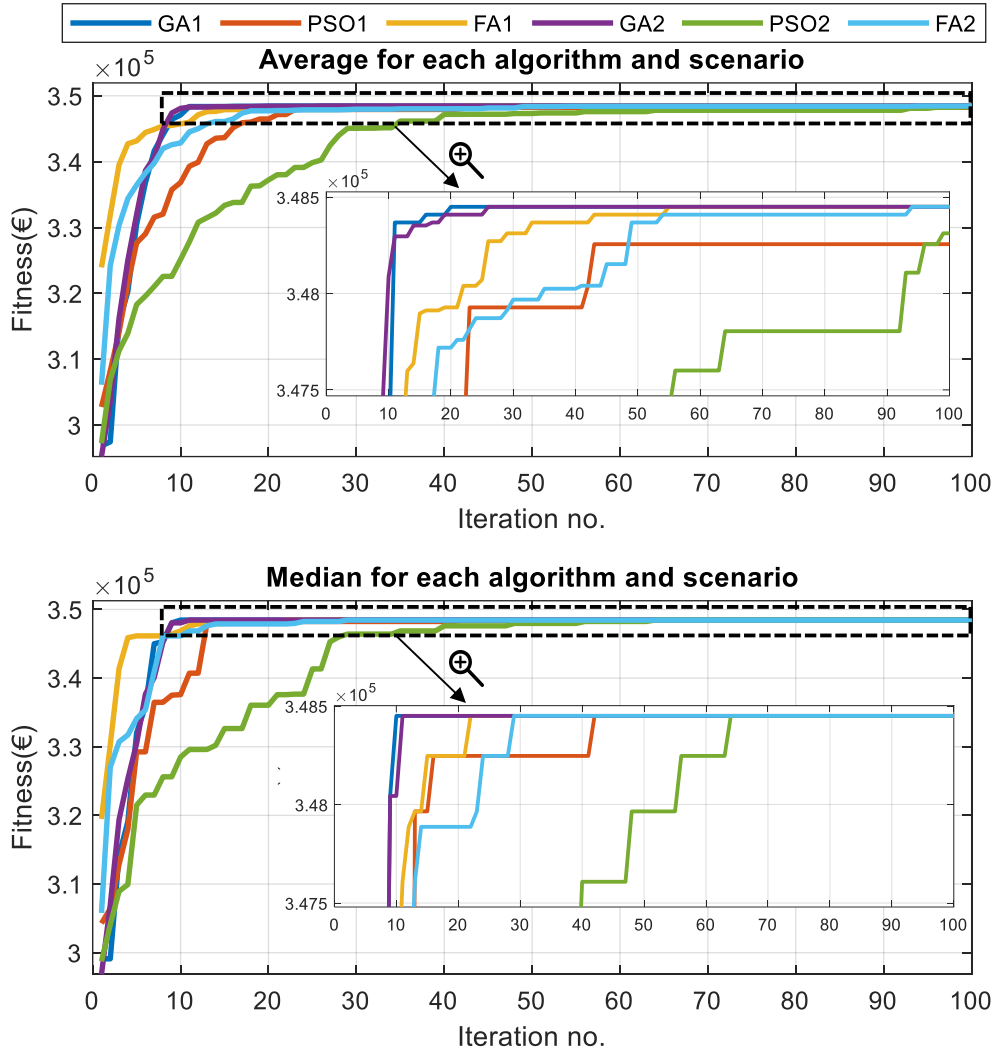
Figure 5: Evolution of the average and median of the fitness functions

The average of the fitness function is very sensitive to "outlier" instances, where the optimum is not reached or a high number of iterations is required to reach it. This high sensitivity results in two effects:

- If just one instance of a case does not reach the optimum fitness (this instance can be considered an "outlier"), the average of all the instances will not reach it.
- Even in the case that all instances reach the optimum, the average will only do it in the iteration where the slowest instance, in terms of speed of convergence, reach the

optimum (this instance can be considered an "outlier" if it is much slower than the rest of the instances of the case).

The median filters these "outliers" to a certain extent and represents what can be considered the "normal" behavior of the algorithm for a given case. Therefore, the presentation of both metrics helps to have a better insight on the algorithms' performance.

As can be seen, the best fitness value achieved by each of the three algorithms is not improved but matched by the other algorithms. Although it is not possible to assure that the algorithms have reached the global optimum- this is only possible with mathematical optimization- it is very likely that they have reached it, since three different algorithms (run each of them ten instances per optimization case and having two optimization cases per algorithm) have reached the same best solution. Besides, the optimization algorithms selected present good exploration features that prevent them from getting "trapped" in local optima.

Regarding the effectiveness of the algorithms, the GA and FA always reach the optimum solution, while the PSO does not reach it in all its instances. This is clear when analyzing the evolution of the average fitness: while this value is stabilized to, approximately, 348450 €, in the two cases of the GA and the FA (GA1, GA2, FA1, FA2), the average obtained in the two cases of the PSO (PSO1, PSO2) is bellow it. Nevertheless, in a "normal" situation, the PSO gets to the optimum solution, as can be seen when analyzing the median: all the cases of all the algorithms stabilize their value to, approximately, 348450 €.

Regarding the speed of convergence of the algorithms, the GA is faster than the FA, which, in turn, is faster than the PSO. This is clearly seen in the vertical evolution of the averages and medians (especially in the medians, as they filter the "outlier" instances): the two cases of the GA are the first to stabilize, then the two cases of the FA and, finally, the two cases of the PSO.
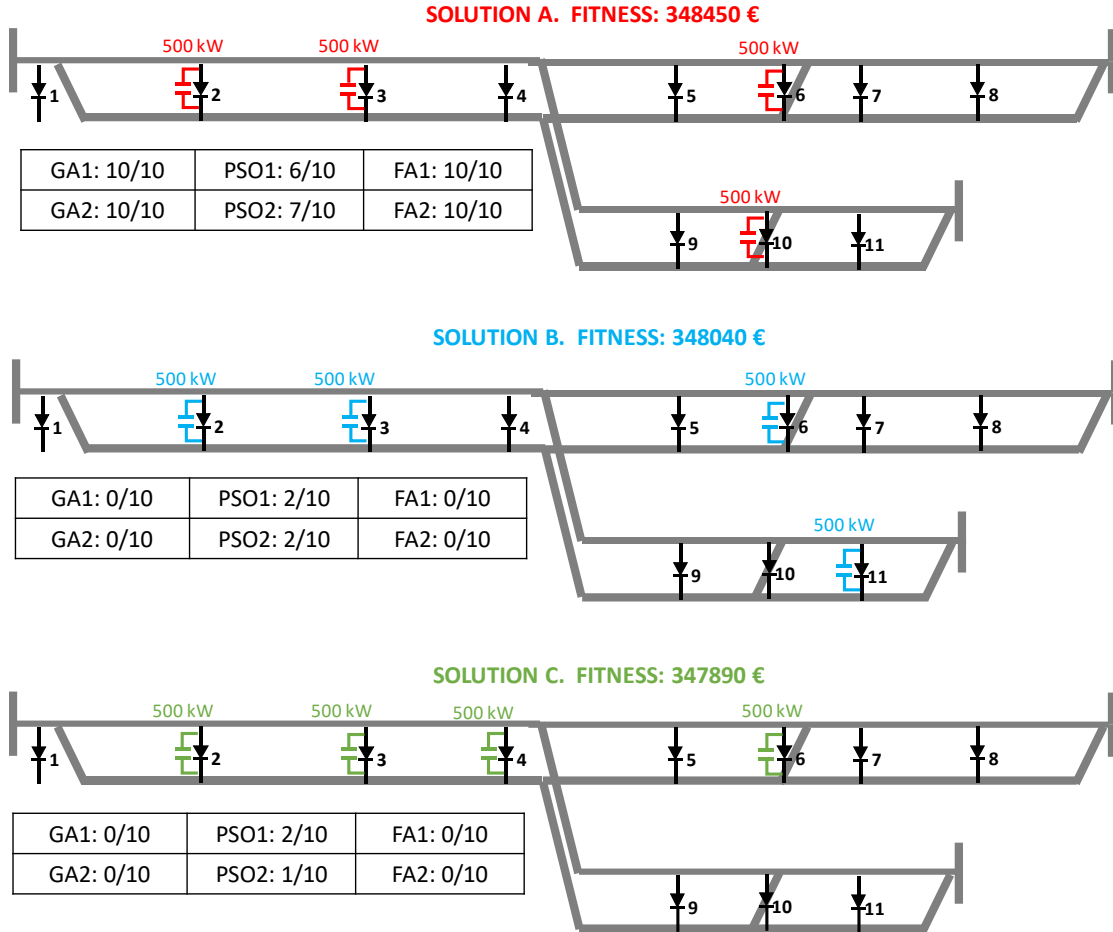
Additionally, the GA and the FA are very robust, as they present a very similar performance in both optimization cases. On the contrary, the PSO is less robust, as its performance is more affected by the optimization cases (it is faster in PSO1 than in PSO2).

In conclusion, the GA presents the best performance, followed by the FA and the PSO.

- The main difference in performance between GA and FA is on the speed of convergence, not in the effectiveness, as both algorithms reach the best solution in all the instances run. The GA requires less iterations to reach the optimum than the FA, although the FA is faster in the initial iterations.
- The PSO is worse than the GA and FA in effectiveness as well as in speed of convergence.

Figure 6 provides the properties (locations and sizes) of the solutions achieved by the algorithms as well as the fitness of the solutions and the number of times (out of the total number of instances) that each algorithm in each optimization case has reached it.

SOLUTION A. FITNESS: 348450 €

| GA1: 10/10 | PSO1: 6/10 | FA1: 10/10 |
| GA2: 10/10 | PSO2: 7/10 | FA2: 10/10 |

SOLUTION B. FITNESS: 348040 €

| GA1: 0/10 | PSO1: 2/10 | FA1: 0/10 |
| GA2: 0/10 | PSO2: 2/10 | FA2: 0/10 |

SOLUTION C. FITNESS: 347890 €

| GA1: 0/10 | PSO1: 2/10 | FA1: 0/10 |
| GA2: 0/10 | PSO2: 1/10 | FA2: 0/10 |

Figure 6: Solutions achieved by the optimization algorithms

When analyzing the solutions, the excellent performance of the optimization algorithms, especially the GA and the FA, has been demonstrated. In pre-optimization tests performed to gain a first understanding of the search space corresponding to the case study line, it was found that the receptivity of the line was reasonably high. Indeed, it was also found that the receptivity is almost absolute (which means that practically the whole amount of regenerated energy is recovered) with installations with a total power greater or equal to 3 MW, The solutions provided by the optimization algorithms are completely in line with the results of these pre-optimization tests, as the total power installed is 2 MW. This means that although there is room to increase the energy savings with a bigger installation (at least until a total power of 3 MW), the marginal benefit from increasing the energy savings does not economically compensate the extra-investment required for it.

Once having analyzed the total amount of power installed, it is also very important to study the distribution of this power among the potential locations where the ESSs can be installed. In the three solutions provided by the algorithms (**Solutions A**, **B** and **C**), the 2 MW of total installed power is very carefully distributed:

- **Solution A** has been achieved in all the instances run with the GA and the FA and in most of the instances run by the PSO. It proposes four locations (each of them with an installation of 500 kW) very carefully chosen: the two central locations of the common section (which all trains must pass through) and the central location of each of the two branches.

- **Solution B** and **Solution C** are only provided by the PSO. They present a slightly worse fitness than **Solution A** and small variations from it. As the total power installed and the number of locations over which it is distributed are the same as in **Solution A**, the only difference is in the locations selected. Concretely, only one location in each of the solutions differ from the locations proposed by **Solution A**:
    - Location 11 instead of 10 (the next location on the same branch) in **Solution B.**
    - Location 4 instead of 10 (the common section increases its number of installations in one ESS to the detriment of branch B-F (the smallest one), which runs out of installations) in **Solution C.**

Finally, it must be noted that from an initial investment of 185400 € (Equation (13) details the calculation of the investment cost for the solutions) the NPV is within 347890 and 348450 €. This implies that the benefit from the installation of the ESSs almost doubles the cost of the initial investment. In particular, the best solution gives a benefit of 188% the initial investment.

$$Install.\,cost\,of\,Solution\,A/B/C = 4 \cdot \left(500\,kW \cdot 90\,\frac{€}{kW} + 5\,kWh \cdot 270\,\frac{€}{kWh}\right) = 185400€ \qquad (13)$$

7. Conclusions

Railway operators of DC-electrified lines have a great interest in improving the electrical infrastructure of these systems in order to increase the energy saving. The installation associated with these improvements involve big investments that need to be adequately assessed. However, the methodology to determine the optimal design of these installations is not sufficiently developed in the scientific literature. This paper proposes a methodology to provide an accurate assessment of the possible infrastructure improvements to undertake in a railway line and determine the optimal installation. It combines the use of a realistic railway simulator and the application of nature-inspired optimization algorithms.

The railway simulator is used to obtain accurate enough energy figures to characterize the energy saving potential of the railway line. It is divided in two main modules:

- The operation module, which represents the real operation of the railway line and models in detail situations of traffic with small and large perturbations.
- The electrical network module, which obtains the electrical information from the traffic scenarios generated by the operation module.

The optimization algorithms perform an intelligent search of the characteristics of the installation, (in terms of number, location and size of the ESSs) that yields the best fitness. The fitness has been defined as the Net Present Value (NPV), as it looks for a balance between energy savings and economic profitability of the investment associated with the infrastructure improvement required to obtain those energy savings.

Three different optimization algorithms have been proposed in order to validate and compare the algorithms' performance as well as the results provided by each of them. The optimization algorithms proposed are the Genetic Algorithm (GA), the Particle Swarm Optimization (PSO) and the Fireworks Algorithm (FA).

The performance of the algorithms is excellent: they combine the reduction of energy consumption with the economic profitability of the investment selected. In particular, results have shown that the GA and the FA have the best performance, the speed of convergence being a bit faster in the case of the GA.

References

[1] Z. Tian *et al*, "System energy optimisation strategies for metros with regeneration," *Transportation Research Part C: Emerging Technologies,* vol. 75, *(Supplement C),* pp. 120-135, 2017. . DOI: https://doi.org/10.1016/j.trc.2016.12.004.

[2] N. Zhao *et al*, "An integrated metro operation optimization to minimize energy consumption," *Transportation Research Part C: Emerging Technologies,* vol. 75, *(Supplement C),* pp. 168-182, 2017. . DOI: https://doi.org/10.1016/j.trc.2016.12.013.

[3] M. Khodaparastan, A. A. Mohamed and W. Brandauer, "Recuperation of Regenerative Braking Energy in Electric Rail Transit Systems," *IEEE Transactions on Intelligent Transportation Systems,* pp. 1-17, 2019.

[4] M. C. Falvo *et al*, "Energy savings in metro-transit systems: A comparison between operational Italian and Spanish lines," *Proceedings of the Institution of Mechanical Engineers, Part F: Journal of Rail and Rapid Transit,* vol. 230, *(2),* pp. 345-359, July 15, 2014.

[5] A. González-Gil, R. Palacin and P. Batty, "Sustainable urban rail systems: Strategies and technologies for optimal management of regenerative braking energy," *Energy Conversion and Management,* vol. 75, pp. 374-388, 11, 2013.

[6] B. Mellitt, Z. Mouneimne and C. Goodman, "Simulation study of DC transit systems with inverting substations," *IEE Proceedings B - Electric Power Applications,* vol. 131, *(2),* pp. 38-50, 1984.

[7] V. Gelman, "Energy Storage That May Be Too Good to Be True: Comparison Between Wayside Storage and Reversible Thyristor Controlled Rectifiers for Heavy Rail," *Vehicular Technology Magazine, IEEE,* vol. 8, *(4),* pp. 70-80, 2013.

[8] H. Ibaiondo and A. Romo, "Kinetic energy recovery on railway systems with feedback to the grid," in *Power Electronics and Motion Control Conference (EPE/PEMC), 2010 14th International,* 2010, pp. T9-94-T9-97.

[9] G. Zhang *et al*, "A new hybrid simulation integrating transient-state and steady-state models for the analysis of reversible DC traction power systems," *International Journal of Electrical Power & Energy Systems,* vol. 109, pp. 9-19, 2019. . DOI: https://doi.org/10.1016/j.ijepes.2019.01.033.

[10] Z. Gao *et al*, "Control of urban rail transit equipped with ground-based supercapacitor for energy saving and reduction of power peak demand," *International Journal of Electrical Power & Energy Systems,* vol. 67, pp. 439-447, 5, 2015.

[11] H. Lee *et al*, "Peak power reduction and energy efficiency improvement with the superconducting flywheel energy storage in electric railway system," *Physica C: Superconductivity,* vol. 494, *(0),* pp. 246-249, 11/15, 2013.

[12] D. Iannuzzi, F. Ciccarelli and D. Lauria, "Stationary ultracapacitors storage device for improving energy saving and voltage profile of light transportation networks," *Transportation Research Part C: Emerging Technologies,* vol. 21, *(1),* pp. 321-337, 4, 2012.

[13] D. Roch-Dupré *et al*, "Analysis of the demand charge in DC railway systems and reduction of its economic impact with Energy Storage Systems," *International Journal of Electrical Power & Energy Systems,* vol. 93, pp. 459-467, 2017. . DOI: https://doi.org/10.1016/j.ijepes.2017.06.022.

[14] M. Khodaparastan *et al*, "Modeling and Simulation of DC Electric Rail Transit Systems With Wayside Energy Storage," *IEEE Transactions on Vehicular Technology,* vol. 68, *(3),* pp. 2218-2228, 2019.

[15] D. Roch-Dupré *et al*, "Evaluation of the impact that the traffic model used in railway electrical simulation has on the assessment of the installation of a Reversible Substation," *International Journal of Electrical Power & Energy Systems,* vol. 102, pp. 201-210, 2018. . DOI: https://doi.org/10.1016/j.ijepes.2018.04.030.

[16] W. Jefimowski and A. Szeląg, "The multi-criteria optimization method for implementation of a regenerative inverter in a 3kV DC traction system," *Electric Power Systems Research,* vol. 161, pp. 61-73, 2018. . DOI: https://doi.org/10.1016/j.epsr.2018.03.023.

[17] F. H. Pereira, C. L. Pires and S. I. Nabeta, "Optimal placement of rectifier substations on DC traction systems," *IET Electrical Systems in Transportation,* vol. 4, *(3),* pp. 62-69, 2014.

[18] C. Hui-Jen *et al*, "Optimization of inverter placement for mass rapid transit systems using genetic algorithm," in Dalian, 2005, pp. 1-6.

[19] H. J. Chuang, "Optimisation of inverter placement for mass rapid transit systems by immune algorithm," *IEE Proceedings - Electric Power Applications,* vol. 152, *(1),* pp. 61-71, 2005.

[20] Á J. López-López, "Optimising the Electrical Infrastructure of Mass Transit Systems to Improve the use of Regenerative Braking." , PhD Thesis. Universidad Pontificia Comillas, 2016.

[21] V. Calderaro *et al*, "Optimal siting and sizing of stationary supercapacitors in a metro network using PSO," in *Industrial Technology (ICIT), 2015 IEEE International Conference On,* 2015, pp. 2680-2685.

[22] H. Xia *et al*, "Optimal energy management, location and size for stationary energy storage system in a metro line based on genetic algorithm," *Energies,* vol. 8, *(10),* pp. 11618-11640, 2015.

[23] B. Wang *et al*, "An Improved Genetic Algorithm for Optimal Stationary Energy Storage System Locating and Sizing," *Energies,* vol. 7, *(10),* pp. 6434, 2014.

[24] T. Ratniyomchai, S. Hillmansen and P. Tricoli, "Optimal capacity and positioning of stationary supercapacitors for light rail vehicle systems," in *2014 International Symposium on Power Electronics, Electrical Drives, Automation and Motion,* 2014, pp. 807-812.

[25] T. Ratniyomchai, S. Hillmansen and P. Tricoli, "Energy loss minimisation by optimal design of stationary supercapacitors for light railways," in *2015 International Conference on Clean Electrical Power (ICCEP),* 2015, pp. 511-517.

[26] S. de la Torre *et al*, "Optimal Sizing of Energy Storage for Regenerative Braking in Electric Railway Systems," *IEEE Transactions on Power Systems,* vol. 30, *(3),* pp. 1492-1500, 2015.

[27] D. Roch-Dupré *et al*, "Simulation-based assessment of the installation of a Reversible Substation in a railway line, including a realistic model of large traffic perturbations," *International Journal of Electrical Power & Energy Systems,* vol. 115, pp. 105476, 2020. . DOI: https://doi.org/10.1016/j.ijepes.2019.105476.

[28] S. S. Fazel, S. Firouzian and B. B. Shandiz, "Energy-Efficient Emplacement of Reversible DC Traction Power Substations in Urban Rail Transport through Regenerative Energy Recovery," *International Journal of Railway Research,* vol. 1, *(2),* pp. 11-22, 2014.

[29] C. H. Bae, "A simulation study of installation locations and capacity of regenerative absorption inverters in DC 1500 V electric railways system," *Simulation Modelling Practice and Theory,* vol. 17, *(5),* pp. 829-838, 5, 2009.

[30] H. Xia *et al*, "Optimal Energy Management, Location and Size for Stationary Energy Storage System in a Metro Line Based on Genetic Algorithm," *Energies,* vol. 8, *(10),* pp. 11618-11640, 2015.

[31] M. Mavrovouniotis, C. Li and S. Yang, "A survey of swarm intelligence for dynamic optimization: Algorithms and applications," *Swarm and Evolutionary Computation,* vol. 33, pp. 1-17, 2017. . DOI: https://doi.org/10.1016/j.swevo.2016.12.005.

[32] M. P. Saka, O. Hasançebi and Z. W. Geem, "Metaheuristics in structural optimization and discussions on harmony search algorithm," *Swarm and Evolutionary Computation,* vol. 28, pp. 88-97, 2016. . DOI: https://doi.org/10.1016/j.swevo.2016.01.005.

[33] O. Ertenlice and C. B. Kalayci, "A survey of swarm intelligence for portfolio optimization: Algorithms and applications," *Swarm and Evolutionary Computation,* vol. 39, pp. 36-52, 2018. . DOI: https://doi.org/10.1016/j.swevo.2018.01.009.

[34] A. Fernández-Rodríguez, A. Fernández-Cardador and A. P. Cucala, "Real time eco-driving of high speed trains by simulation-based dynamic multi-objective optimization," *Simulation Modelling Practice and Theory,* vol. 84, pp. 50-68, 2018. . DOI: https://doi.org/10.1016/j.simpat.2018.01.006.

[35] M. Domínguez *et al*, "Optimal design of metro automatic train operation speed profiles for reducing energy consumption," *Proceedings of the Institution of Mechanical Engineers, Part F (Journal of Rail and Rapid Transit),* vol. 225, pp. 463-473, 09/01, 2011.

[36] C. J. Goodman, L. K. Siu and T. K. Ho, "A review of simulation models for railway systems," in *International Conference on Developments in Mass Transit Systems,* London, UK, 1998, pp. 80-85.

[37] I. Martínez *et al*, "Statistical dwell time model for metro lines," *WIT Transactions on the Built Environment,* vol. 96, pp. 1-10, 2007.

[38] Á J. López-López *et al*, "Assessment of energy-saving techniques in direct-current-electrified mass transit systems," *Transportation Research Part C: Emerging Technologies,* vol. 38, pp. 85-100, 01, 2014.

[39] D. E. Goldberg and J. H. Holland, "Genetic algorithms and machine learning," *Mach. Learning,* vol. 3, *(2),* pp. 95-99, 1988.

[40] J. Kennedy and R. C. Eberhart, "Particle swarm optimization," in *Neural Networks, 1995. Proceedings., IEEE International Conference On,* 1995, pp. 1942-1948 vol.4.

[41] Y. Tan and Y. Zhu, "Fireworks algorithm for optimization," in *International Conference in Swarm Intelligence,* 2010, pp. 355-364.

[42] Q. Long *et al*, "A genetic algorithm for unconstrained multi-objective optimization," *Swarm and Evolutionary Computation,* vol. 22, pp. 1-14, 2015. . DOI: https://doi.org/10.1016/j.swevo.2015.01.002.

[43] N. Lynn and P. N. Suganthan, "Heterogeneous comprehensive learning particle swarm optimization with enhanced exploration and exploitation," *Swarm and Evolutionary Computation,* vol. 24, pp. 11-24, 2015. . DOI: https://doi.org/10.1016/j.swevo.2015.05.002.

[44] L. He *et al*, "A discrete multi-objective fireworks algorithm for flowshop scheduling with sequence-dependent setup times," *Swarm and Evolutionary Computation,* pp. 100575, 2019. . DOI: https://doi.org/10.1016/j.swevo.2019.100575.

[45] T. Gonsalves, *Artificial Intelligence: A Non-Technical Introduction* . Sophia University Press, 2017.

[46] Á J. López-López *et al*, "Improving the Traffic Model to Be Used in the Optimisation of Mass Transit System Electrical Infrastructure," *Energies,* vol. 10, *(8),* pp. 1134, 2017.

[47] Á J. López-López *et al*, "Smart traffic-scenario compressor for the efficient electrical simulation of mass transit systems," *International Journal of Electrical Power & Energy Systems,* vol. 88, pp. 150-163, 6, 2017.

[48] J. Xin, G. Chen and Y. Hai, "A Particle Swarm Optimizer with Multi-stage Linearly-Decreasing Inertia Weight," *2009 International Joint Conference on Computational Sciences and Optimization,* vol. 1, pp. 505-508, 2009.

[49] P. Ralon *et al*, "Electricity storage and renewables: costs and markets to 2030," *International Renewable Energy Agency: Abu Dhabi, UAE,* 2017.